Supporting Information

Yesilaltay et al. 10.1073/pnas.1418954111

SI Materials and Methods

Animals. All animals were maintained on an RMH3000 laboratory diet ad libitum. All animal experiments were performed in accordance with the committees for animal care guidelines from the Massachusetts Institute of Technology and the School of Medicine of Pontificia Universidad Católica de Chile. The *SR-BI*$^{+/-}$ and *SR-BI*$^{-/-}$ mice were offspring of mice that had been derived from F1 hybrids (50% contributions from C57BL/6 and 129) and thus, have a 50:50 C57BL/6:129 mixed genetic background (1). WT mice on a pure C57BL/6 background were purchased from Charles River Laboratories, Jackson Laboratory, or Taconic. Typically, oocytes or eggs were isolated from two to six female donors of each genotype, with four to six donors used in most experiments. The yields of eggs per donor varied from 10 to 40, and typically, they were ∼20–30 eggs.

Oocyte and Follicle Diameter Measurements. To analyze oocyte and follicle growth in vivo, follicles at various sizes were isolated from unprimed, sexually immature 3-wk-old and mature 6-wk-old female *SR-BI*$^{+/-}$ and SR-BI KO mice as previously described (2, 3). Ovaries were teased by a 27-gauge needle under a stereomicroscope in Hepes-buffered MEM with Hanks' salts (Life Technologies; Gibco BRL) containing 0.3% BSA and antibiotics (100 IU/mL penicillin and 100 μg/mL streptomycin). After isolation, follicles were fixed at 37 °C for 30 min in microtubule stabilizing buffer [0.1 M Pipes, pH 6.9, 5 mM $MgCl_20.6H_2O$, 2.5 mM EGTA containing 2% (wt/vol) formaldehyde, 0.1% Triton X-100, 1 mM Taxol, 10 U/mL aprotinin, 50% (vol/vol) deuterium oxide] (4). Diameters of fixed oocytes and follicles were measured by an inverted scope equipped with a CCD camera using Spot Software and calibrated by a micrometer. The follicle and oocyte diameters were determined by making two measurements, the second of which was made at right angle to the first measurement. The averages of these two values were expressed as the diameter of the oocyte and the follicle in Fig. 2. Numbers of follicles used in the study were $n = 49$ for *SR-BI*$^{+/-}$ and $n = 50$ for SR-BI KO 3-wk-old animals and $n = 89$ for *SR-BI*$^{+/-}$ and $n = 107$ for SR-BI KO 6-wk-old animals. Graphs and linear curve fitting were generated by Microsoft Excel.

In Vitro Maturation of Oocytes. Oocyte maturation is the process by which an oocyte arrested in MI resumes and completes the first meiotic division I (5). Oocytes at the GV stage that were surrounded by cumulus cells were collected from unprimed 6- to 8-wk-old female mice after follicular puncture in collection medium. Oocytes were then cultured for 14 h in basal in vitro maturation medium consisting of MEM with Earle's salts (Gibco Invitrogen Life Technologies), 2 mM glutamine, 0.23 mM pyruvate, 100 IU penicillin, 100 mg/mL streptomycin, and 0.3% BSA at 37 °C under 5% (vol/vol) CO_2 as previously described (6). At the end of the incubation period, cumulus cells were dispersed by gentle pipetting, and oocytes were fixed in microtubule stabilizing buffer and placed in storage buffer containing 2% (wt/vol) BSA, 2% (wt/vol) powder milk, 2% (vol/vol) normal goat serum, 0.1 M glycine, and 0.01% (vol/vol) Triton X-100 and kept at 4 °C. Then, oocytes were incubated with Hoechst 33258 dye to analyze DNA and assessed using a fluorescence microscope for meiotic maturation (extrusion of the first PB). To study the kinetics of oocyte maturation, oocytes were obtained by follicular puncture from pregnant mare serum gonadotropin (PMSG) -primed females in M16 medium supplemented with 0.3% BSA and antibiotics and containing 3-isobutyl-1-methylxanthine at 200 μM. Cumulus cells were removed by serial aspiration through a fine-bore pipette. Denuded oocytes were then transferred to 3-isobutyl-1-methylxanthine–free M16 medium and cultured at 37 °C under 5% (vol/vol) CO_2 to initiate maturation. Oocyte maturation was determined as a function of time by inspection of GVBD using an inverted microscope (Nikon TMS; Nikon) at 200× magnification.

Isolation of Ovulated Eggs. Six- to twelve-week-old WT C57BL/6, *SR-BI*$^{+/+}$, *SR-BI*$^{+/-}$, and SR-BI KO (*SR-BI*$^{-/-}$) female mice received 0.1-mL i.p. injections of PMSG (5 IU) and 46–48 h later, 0.1 mL hCG (5 IU) to induce superovulation; 14–20 h after hCG injection, oocyte cumulus complexes were collected from the oviductal ampullae and treated with hyaluronidase (150 μg/mL) in FHM (MR-025-D; Millipore Corp.) or M2 medium for 5–10 min to disperse cumulus cells. Only viable oocytes were collected; oocytes at harvest that were categorized as dead by analysis of their morphologies (flat and darkened appearance) using a stereomicroscope were discarded. In some experiments, Trypan Blue staining was used to confirm cell death. On average, 4% of oocytes (median = 0%, $n = 47$ animals) from *SR-BI*$^{+/-}$ animals and 19% of oocytes (median = 18%, $n = 39$ animals) obtained from SR-BI KO animals were dead. Collected oocytes were washed three times and kept in M16 medium at 37 °C in a 5% (vol/vol) CO_2 incubator for 20–60 min until processed further.

Egg Activation by $SrCl_2$ and Cholesterol Loading. Hyaluronidase-treated eggs were washed three times in M16 medium. Unless indicated otherwise, for activation with $SrCl_2$, eggs were incubated for 6 h at 37 °C in M16 medium containing 5 mM $SrCl_2$ and 2 mM EGTA. Unless indicated otherwise, for cholesterol loading, eggs were placed in M16 medium containing 0.125 or 0.5 mM cholesterol-loaded MβCD (Sigma or CTD, Inc.) for 10, 15, or 25 min at 37 °C as indicated and then washed three times in M16. [For intracellular calcium imaging experiments, phenol red-free M2 medium was used instead of M16 medium (see details below).] Typically, eggs were incubated for an additional 5–6 h in M16 at 37 °C and then scored for viability and extrusion of second PBs. In some experiments, the eggs were then harvested and pooled for kinase activity assays or subjected to whole-mount staining and deconvolution microscopy. In other experiments, the eggs were cultured for an additional ∼18 h at 37 °C in M16 or phenol red-free M2 media and then scored for cleavage to the two-cell stage.

Filipin Staining and Microscopy. Ovulated eggs were collected from female mice subjected to 0.10-mL i.p. injections of PMSG (5 IU) and 46–48 h later, 0.1 mL hCG (5 IU) to induce superovulation. Eggs were collected ∼16 h after administration of hCG and treated with hyaluronidase as described above to remove cumulus cells. Viable eggs were washed in M16 medium and then fixed in 4% (wt/vol) paraformaldehyde in PBS overnight at 4 °C. They were then washed three times in PBS, incubated in 0.5 mg/mL Filipin III complex (Sigma) in PBS for 1 h at room temperature, washed two times with PBS, mounted on slides using Fluoromount G immunofluorescence mounting medium (Electron Microscopy Sciences) and a coverslip, and then, imaged under UV light (excitation = 380–450 nm and emission = 450–490 nm) using a fluorescence microscope (Zeiss Int.). Comparable results were obtained when oocytes were fixed in microtubule stabilizing buffer (composed of 0.1 M Pipes, pH 6.9, 5 mM $MgCl_20.6H_2O$, 2.5 mM EGTA) containing 2% (wt/vol)

formaldehyde, 0.1% Triton X-100, 1 μM Taxol, 10 U/mL aprotinin, and 50% (vol/vol) deuterium oxide for 30 min at 37 °C. The relative intensities of fluorescence of filipin-stained eggs from *SR-BI*$^{+/+}$ mice (n = 6 untreated eggs and n = 6 cholesterol-loaded eggs) and SR-BI KO mice (n = 7 untreated eggs) from two independent experiments were quantified using Image J software (7).

Whole-Mount Staining and Deconvolution Microscopy. Ovulated eggs were collected and pooled from PMSG- and hCG-treated (superovulated) females (three to five donor females per genotype per group) either ∼16 or ∼20 h post-hCG administration and denuded by hyaluronidase treatment as described above. We included the long ∼20-h post-hCG samples in our analysis, because these samples uncovered a time dependence in the escape of SR-BI KO oocytes from MII arrest, exhibiting a greater fraction escaping MII arrest at the longer time without a dramatic change in the phenotype of the eggs from control animals. Cumulus-free eggs were washed two times in PBS supplemented with 0.1% polyvinylpyrrolidone, fixed for 45 min in 4% (wt/vol) paraformaldehyde, permeabilized in 0.1% Triton X-100, and blocked with 10% (vol/vol) donkey serum for 20 min as previously described (8). The eggs were then stained with the following antibodies. Monoclonal rat antitubulin (YL/2; ab6160; Abcam) and polyclonal rabbit antilamin B1 antibodies (ab16048; Abcam) were used at a 1:250 dilution. Human anticentromere antibody (15–234-0001; Antibodies, Inc.) was used at a 1:100 dilution. After staining, the eggs were mounted on slides with Vectashield mounting medium containing DAPI (Vector Labs) with a 3:1 paraffin:petroleum jelly mixture used as a spacer between the coverslip and the slide to preserve the 3D structures of the eggs. Images (z stacks collected at 0.5-μm spacing) were recorded using a DeltaVision deconvolution microscope (AppliedPrecision). All images within the stacks were deconvolved using AppliedPrecision softWoRx software. z-Stack projections were generated using the maximum intensity method (9) in ImageJ (7) or AppliedPrecision softWoRx software.

In Vitro Determination of MPF and MAPK Activities. We based our procedure on previously described MPF and MAPK assays (10, 11) and a protocol generously provided by R. Fissore and C. He (University of Massachusetts, Amherst, MA). Reagents were purchased from Sigma-Aldrich unless otherwise indicated. In brief, eggs were harvested from the oviducts of hormone-primed females either ∼14–16 (C57BL/6 background; four donors per harvest per day) or 18 h (mixed C57BL/6:129 background; one or two donors per genotype per harvest per experiment for two independent experiments) after hCG administration. Eggs were subjected to treatment without or with cholesterol/MβCD (CTD, Inc.) or $SrCl_2$/EGTA, incubated for 6 h at 37 °C as described above, and washed three times with M16 medium, and pools of four oocytes in ∼0.5 μL M16 medium were transferred into 1.5-mL snap-cap tubes containing 4.5 μL kinase buffer (80 mM glycerophosphate, 20 mM EGTA, 15 mM $MgCl_2$, 1 mM DTT, 10 μg/mL aprotinin, 10 μg/mL leupeptin, 10 μg/mL pepstatin, 2 μg/mL cAMP-dependent protein kinase inhibitor; ALX-165-024; Enzo), lysed by six rounds of freezing in liquid nitrogen and thawing in a 37 °C water bath, and stored at −80 °C until use. The kinase activities were determined by adding to each thawed lysate 5 μL kinase reaction buffer [1.3 μg/μL histone H1 (type III-S; MPF substrate), 0.2 μg/μL myelin basic protein (MBP; MAPK substrate), 0.4 mM unlabeled ATP, 2 μCi [γ-^{32}P] ATP; Perkin-Elmer] followed by incubation at 25 °C for 30 min. For negative controls, ∼0.5 μL M16 medium containing four eggs was replaced by 0.5 μL M16 medium without eggs. The two kinase reactions proceeded simultaneously in each assay tube and were terminated by adding 10 μL 2× Laemmli sample buffer (Bio-Rad) and immersing the samples for 3 min in boiling water. The denatured samples and prestained size markers (Bio-Rad) were then subjected to electrophoresis using 8–16% gradient mini-PROTEAN TGX Gel (Bio-Rad) gels. The relative amounts of ^{32}P incorporated into the histone H1 and MBP substrates were determined by exposing the gels on a phosphor storage screen (GE) and measuring the intensities using a Typhoon FLA 9500 laser scanner (GE Healthcare Life Sciences) made available by Michael Laub and Tania Baker (Biology Department, Massachusetts Institute of Technology, Cambridge, MA). The intensities of the bands in each lane representing both histone H1 (∼30–32 kDa) and MBP (∼21.5 kDa) were quantified using the Fiji software package (fiji.sc/Fiji) and analyzed using Matlab. For each individual gel, the intensities of the bands representing histone H1 and MBP were corrected by subtracting the corresponding background intensities from the negative control lane (no eggs). Each gel included two to four replicates of pools of untreated WT C57BL/6 or *SR-BI*$^{+/+}$ eggs, and the mean intensities for histone H1 and MBP bands in these samples were defined as 100% and used to calculate the relative intensities of the bands for the other samples on the same gel. The relative intensities for equivalent samples (same genotypes and treatments) from multiple independent gels were averaged after normalization to the 100% controls.

Intracellular Calcium Imaging. We based our procedure on previously described assays (11, 12) and a protocol generously provided by R. Fissore and C. He (University of Massachusetts, Amherst, MA). Eggs were maintained at 37 °C in drops of the indicated media covered by mineral oil unless otherwise noted. Eggs isolated from the oviducts of hormone-primed WT C57BL/6 females ∼14–16 h after hCG administration were denuded by hyaluronidase treatment. The eggs were divided into three batches of ∼20 eggs each, and each batch was processed separately as described below. Typically, processing of the first batch of eggs began ∼1.5 h after hyaluronidase treatment, and processing of the last batch began ∼4.5 h after hyaluronidase treatment. We noted reduced efficiency of activation (<45% activated eggs) by cholesterol/MβCD when processing began >5 h after hyaluronidase treatment. We excluded from our analysis results for eggs from individual batches in which the fraction of eggs induced to extrude PBs by cholesterol/MβCD was <45% (greater than 2 SDs away from the mean). Eggs were loaded with a calcium-sensitive fluorescent dye by incubation for 0.5–1 h at room temperature in the dark with 4 μM Fura-2AM (prepared from a fresh 1 mM stock solution in DMSO; Life Technologies) and 0.04% pluronic acid (Life Technologies) in Hepes-buffered phenol red-free M2 medium. All M2 used in the calcium imaging experiments was phenol red-free. The M2 contained 2.0 mM Ca^{2+} unless otherwise indicated.

We used the well-established activating agent $SrCl_2$ to validate our method of detecting $[Ca^{2+}]_i$ in activated eggs. Eggs were washed three times with 5 mM $SrCl_2$ in Ca^{2+}-free M2 and then placed in clusters of 4–17 eggs into 60-mm glass-bottom dishes (MatTek Corp.) containing 5 mM $SrCl_2$ in Ca^{2+}-free M2 for imaging. Typically, 2–5 min were required to position and focus on the eggs before the start of data acquisition. Images were collected using a DeltaVision Applied Precision Inc. microscope equipped with 4× and 10× objectives, excitation and emission filter wheels, a 100 W Mercury lamp, a Photometrics Cool SNAP HQ2 camera, Applied Precision Sofworx software, and an environmental chamber maintained at 37 °C. During data acquisition for 30–45 min, samples were excited sequentially every 5, 10, or 60 s at wavelengths of 340 and 380 nm (0.8–1.5 s each), and the emitted light was collected at 526/38 nm as 2D images. An example of the oscillations seen when imaging $SrCl_2$-treated eggs using this method is shown in Fig. S5 together with an untreated control egg that exhibited baseline relative $[Ca^{2+}]_i$. The shape of each spike in the $SrCl_2$-treated egg is similar to that

previously reported for $SrCl_2$-mediated activation (13, 14). After imaging (~1 h after dye loading), the eggs were transferred to a new dish containing the same medium and cultured in a 5% (vol/vol) CO_2 incubator for an additional ~5–24 h. Cells were examined for PB extrusion at 5–7 h after imaging and in some cases, cleavage at ~24 h.

For cholesterol activation, eggs were washed three times with M2 containing 0.125 mM cholesterol/MβCD and then placed in clusters of 4–17 eggs into 60-mm glass-bottom dishes in 0.125 mM cholesterol/MβCD M2 for imaging as described above. Imaging data were collected for either 18–22 min for those eggs exposed to cholesterol/MβCD for only 25 min or 37–40 min for those eggs continuously exposed to cholesterol/MβCD for 45 min. The eggs were then transferred to cholesterol/MβCD-free M2 (transfer time ~ 1 min) and washed three times with M2. For eggs exposed to cholesterol for 25 min, four to six of the eggs in each batch were returned to the microscope for either an additional 15 min of imaging in M2 (a total of 32 eggs in multiple independent experiments were subjected to this two-step imaging protocol) (Fig. S6*A*) or an additional ~150 min of imaging (excitation every 60 s; Fig. S6*B*) in M2 followed by determination of second PB extrusion (20 eggs in three independent experiments were examined, and 2 eggs died during the 150-min imaging period). Imaging data could not be collected during the 5–7 min required to transfer, wash, position, and refocus on the eggs. At the end of the second 15-min period of imaging, the eggs were washed three times with M2, transferred to a new dish containing M2, and cultured for an additional ~5–24 h to assess PB extrusion and cleavage as noted above; 3 of the eggs exposed to cholesterol/MβCD for 25 min and subjected to two-step imaging (3 of 32) were not included in the analyses, because they were dead at 24 h. Two of these exhibited abnormal morphologies (two large cells each) at 6 h. The eggs exposed to cholesterol/MβCD for 45 min in two independent experiments also were cultured in cholesterol/MβCD-free M2 medium for an additional ~5.25 h, after which PB extrusion was assessed. Of 28 eggs exposed to cholesterol/MβCD for 45 min, 1 egg died during the imaging, and 1 egg died before the end of the additional ~5.25 h of incubation. Of the remaining 26 eggs, 20 eggs exhibited second PB extrusion. Some of the Fura-2AM-labeled eggs treated with $SrCl_2$ or cholesterol/MβCD were not imaged but were examined for PB extrusion and cleavage as indicated above. In some experiments, untreated control eggs were processed identically to either the $SrCl_2$- or cholesterol/MβCD-treated eggs. We observed no increases in relative $[Ca^{2+}]_i$ in the untreated control eggs.

The fluorescence images were saved as .tif files. The boundaries of the cells in each image were preliminarily determined using the Auto Threshold and Select Particle functions of Fiji software (fiji.sc/Fiji) and adjusted manually when necessary. This software was then used to calculate the total cell fluorescence intensities at 340 and 380 nm. For each cell, a corresponding cell-free area in each image was used to calculate the background fluorescence intensities for that cell. Matlab and Excel software were used to calculate the relative $[Ca^{2+}]_i$ for each cell in each image as follows:

$$\text{relative}\left[Ca^{2+}\right]_i = \frac{\text{total cell intensity (340 nm)} - \text{background (340 nm)}}{\text{total cell intensity (380 nm)} - \text{background (380 nm)}} \times \frac{\text{exitation time (380 nm)}}{\text{exitation time (340 nm)}} \times \frac{\text{ND transmitted (380 nm)}}{\text{ND transmitted (340 nm)}} \times 1{,}250,$$

where ND transmitted represents the fraction of emitted light transmitted through a neutral density filter (typically 1.0 for 340 nm and 0.1 for 380 nm) . The excitation times were 1.0 s for 340 nm and 0.8 s for 380 nm. We multiplied values by 1,250 to normalize the control relative $[Ca^{2+}]_i$ to ~2.

Statistical Analysis. The statistical significance of the differences was determined by one-way ANOVA and Tukey posthoc test, Student *t* test, or nonparametric Wilcoxon test. Average values were shown ± SEM. Differences were considered significant when $P < 0.05$.

1. Rigotti A, et al. (1997) A targeted mutation in the murine gene encoding the high density lipoprotein (HDL) receptor scavenger receptor class B type I reveals its key role in HDL metabolism. *Proc Natl Acad Sci USA* 94(23):12610–12615.
2. Carabatsos MJ, Sellitto C, Goodenough DA, Albertini DF (2000) Oocyte-granulosa cell heterologous gap junctions are required for the coordination of nuclear and cytoplasmic meiotic competence. *Dev Biol* 226(2):167–179.
3. Carabatsos MJ, Elvin J, Matzuk MM, Albertini DF (1998) Characterization of oocyte and follicle development in growth differentiation factor-9-deficient mice. *Dev Biol* 204(2):373–384.
4. Messinger SM, Albertini DF (1991) Centrosome and microtubule dynamics during meiotic progression in the mouse oocyte. *J Cell Sci* 100(Pt 2):289–298.
5. Li R, Albertini DF (2013) The road to maturation: oSmatic cell interaction and self-organization of the mammalian oocyte. *Nat Rev Mol Cell Biol* 14(3):141–152.
6. Sanfins A, Lee GY, Plancha CE, Overstrom EW, Albertini DF (2003) Distinctions in meiotic spindle structure and assembly during in vitro and in vivo maturation of mouse oocytes. *Biol Reprod* 69(6):2059–2067.
7. Schneider CA, Rasband WS, Eliceiri KW (2012) NIH Image to ImageJ: 25 years of image analysis. *Nat Methods* 9(7):671–675.
8. Endo T, Naito K, Aoki F, Kume S, Tojo H (2005) Changes in histone modifications during in vitro maturation of porcine oocytes. *Mol Reprod Dev* 71(1):123–128.
9. Agard DA (1984) Optical sectioning microscopy: Cellular architecture in three dimensions. *Annu Rev Biophys Bioeng* 13:191–219.
10. Fissore RA, He CL, Vande Woude GF (1996) Potential role of mitogen-activated protein kinase during meiosis resumption in bovine oocytes. *Biol Reprod* 55(6):1261–1270.
11. Gordo AC, Kurokawa M, Wu H, Fissore RA (2002) Modifications of the Ca^{2+} release mechanisms of mouse oocytes by fertilization and by sperm factor. *Mol Hum Reprod* 8(7):619–629.
12. Cheon B, Lee HC, Wakai T, Fissore RA (2013) Ca^{2+} influx and the store-operated Ca^{2+} entry pathway undergo regulation during mouse oocyte maturation. *Mol Biol Cell* 24(9):1396–1410.
13. Zhang D, et al. (2005) Strontium promotes calcium oscillations in mouse meiotic oocytes and early embryos through InsP3 receptors, and requires activation of phospholipase and the synergistic action of InsP3. *Hum Reprod* 20(11):3053–3061.
14. Wakai T, Zhang N, Vangheluwe P, Fissore RA (2013) Regulation of endoplasmic reticulum $Ca^{(2+)}$ oscillations in mammalian eggs. *J Cell Sci* 126(Pt 24):5714–5724.

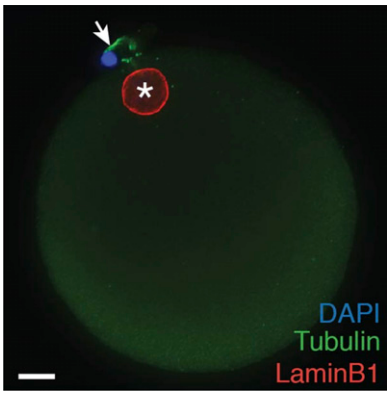

Fig. S1. Visualization of spontaneous pronucleus formation in SR-BI KO eggs. Eggs were harvested from SR-BI KO females ~20 h after hCG administration (induction of superovulation) and denuded by hyaluronidase treatment. The eggs were stained to visualize chromosomes (DAPI; blue), microtubules (tubulin; green), centromeres (anticentromere antibody) (Fig. 3), and the nuclear membrane (lamin B1; red). Deconvolved and *z*-projected images were collected. A representative image of an egg with a lamin B1-stained pronucleus (asterisk) is shown. The arrow indicates the second PB. (Scale bar: 10 μm.)

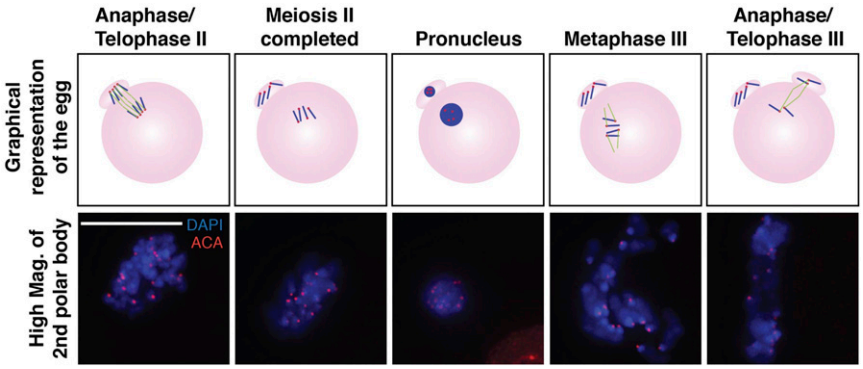

Fig. S2. Visualization of spontaneously formed second PBs in SR-BI KO eggs. Eggs were harvested from SR-BI KO females ~20 h after hCG administration and denuded by hyaluronidase treatment. The eggs were stained to visualize chromosomes (DAPI; blue), microtubules (tubulin) (Fig. 3), centromeres [anti-centromere antibody (ACA); red], and the nuclear membrane (lamin B1) (Fig. S1). Deconvolved and *z*-projected images were collected. Representative images of PBs from eggs at various stages of meiosis (schematically indicated in *Upper*) are shown. The images shown here are from the same eggs shown in Fig. 3. The presence of only 20 chromatids (measured by counting ACA staining puncta) confirms that the observed PBs were second PBs (first PBs would contain 40 chromatids). (Scale bar: 10 μm.)

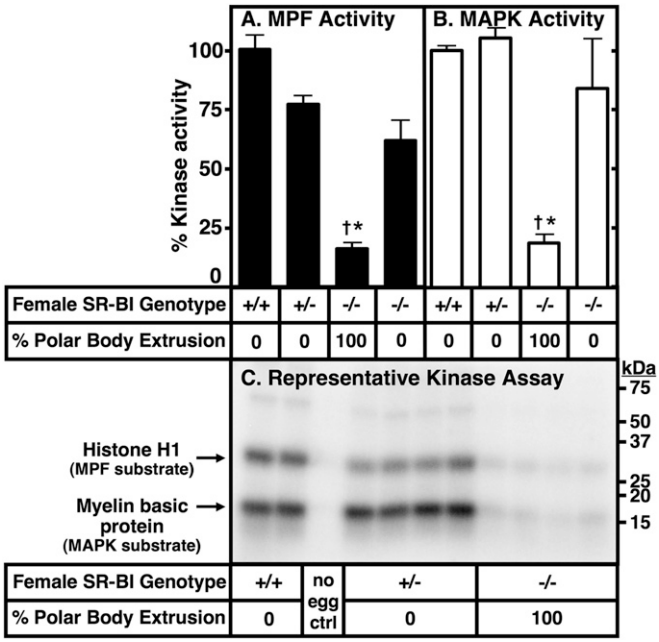

Fig. S3. MPF and MAPK activities of ovulated eggs from control and SR-BI KO mice. Ovulated eggs were harvested from *SR-BI*$^{+/+}$, *SR-BI*$^{+/-}$, and SR-BI KO (SR-BI$^{-/-}$) females ~18 h after hCG administration (induction of superovulation), denuded by hyaluronidase treatment, and incubated for 6 h in M16 medium at 37 °C. The eggs were washed and pooled into sets of four eggs each: *SR-BI*$^{+/+}$, five pools; *SR-BI*$^{+/-}$, seven pools; and *SR-BI*$^{-/-}$ (KO), nine pools. None of the eggs from the *SR-BI*$^{+/+}$ and *SR-BI*$^{+/-}$ mice exhibited second PBs (0%), whereas second PBs were observed in some of the SR-BI KO eggs (100% of eggs in six pools) but not in other SR-BI KO eggs (all eggs in three pools; 0%). Relative (*A*) MPF and (*B*) MAPK activities were determined as incorporation of ^{32}P from [γ-^{32}P]ATP into the MPF substrate histone H1 (~30–32 kDa) and the MAPK substrate MBP (~21.5 kDa) as described in *SI Materials and Methods*. The values for one-way ANOVA for MPF and MAPK activities were $P < 0.002$. *P value < 0.0001 for comparisons with *SR-BI*$^{+/-}$; †P value < 0.0001 (unpaired Student t test) for comparisons with *SR-BI*$^{+/+}$. *C* shows an autoradiograph from the assay used to calculate the values in *A* and *B* (*SI Materials and Methods*). The no egg ctrl lane represents a control sample that did not contain eggs.

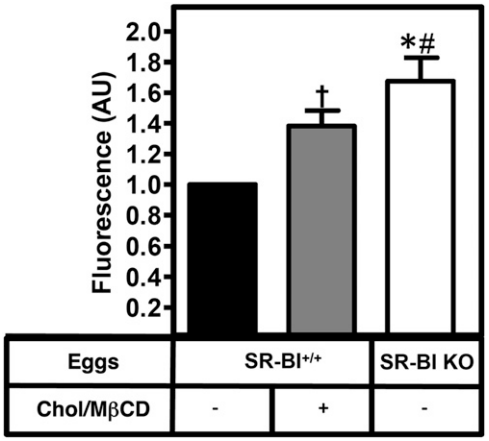

Fig. S4. Relative levels of cholesterol in eggs determined by filipin fluorescence. Oocytes were harvested from *SR-BI*$^{+/+}$ and SR-BI KO females ~16 h after hCG administration (induction of superovulation) and denuded by hyaluronidase treatment. *SR-BI*$^{+/+}$ eggs were incubated for 10 min at 37 °C in either M16 medium alone ($n = 6$ eggs imaged) or M16 containing 0.5 mM cholesterol/MβCD (Chol/MβCD; $n = 6$). Eggs from SR-BI KO mice ($n = 7$) were not treated with Chol/MβCD. All eggs were then fixed, washed, stained by incubation with 0.5 mg/mL Filipin III complex in PBS for 1 h at room temperature, washed, and imaged by fluorescence microscopy as described in *SI Materials and Methods* (above). Bars represent the means ± SEMs in arbitrary units (AUs) relative to the fluorescence intensity of the untreated *SR-BI*$^{+/+}$ control that was defined as 1.0 in each experiment. The value for one-way ANOVA analysis of all samples was $P = 0.0026$, with SR-BI KO eggs exhibiting a significantly higher filipin fluorescence level compared with the untreated *SR-BI* $^{+/+}$ control (68% increase). *SR-BI*$^{+/+}$ eggs treated with Chol/MβCD showed a 38% increase in fluorescence compared with untreated *SR-BI*$^{+/+}$ cells. *$P = 0.004$ for one-sample Student t test; †$P = 0.019$ for Student t test; #$P < 0.001$ for posthoc Tukey test.

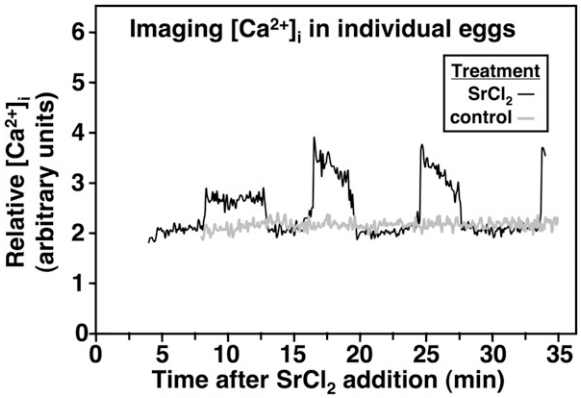

Fig. S5. $SrCl_2$-induced oscillations in $[Ca^{2+}]_i$ in a WT C57BL/6 egg. Eggs isolated from the oviducts of hormone-primed WT C57BL/6 females ~14–16 h after hCG administration were denuded by hyaluronidase treatment. The eggs were loaded with the calcium-sensitive fluorescent dye Fura-2AM. For $SrCl_2$ activation, eggs were placed at time = 0 in Ca^{2+}-free M2 medium supplemented with 5 mM $SrCl_2$ at 37 °C for the duration of the experiment. Untreated control eggs were also examined. Relative $[Ca^{2+}]_i$ was measured with an inverted microscope as a function of time as the ratio of fluorescence intensities excited by 340- and 380-nm light (details in *SI Materials and Methods*). Data for individual $SrCl_2$-treated (black line) and untreated control (light gray line) eggs are shown.

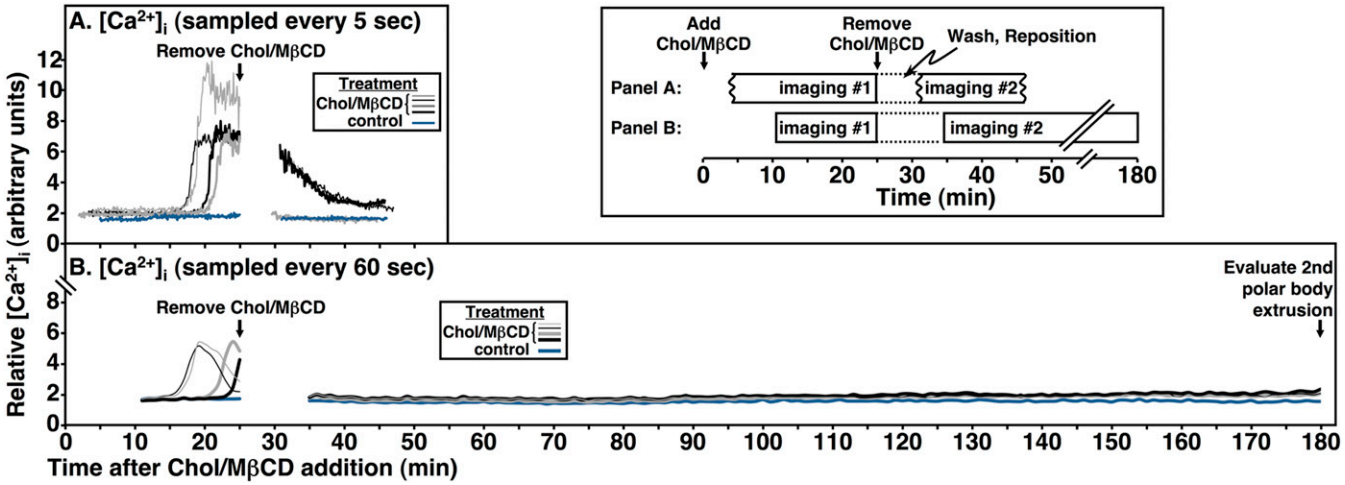

Fig. S6. Effects of cholesterol loading for 25 min on the relative $[Ca^{2+}]_i$ of eggs from WT C57BL/6 females. Eggs from WT C57BL/6 females were harvested ~14–16 h after hCG administration, stripped of cumulus cells by hyaluronidase treatment, and loaded with the calcium-sensitive fluorescent dye Fura-2AM. At time = 0, the eggs were placed in M2 medium supplemented with (treated) or without (control) 0.125 mM cholesterol/MβCD (Chol/MβCD) at 37 °C. A diagram of the experimental protocols is shown in the box in the upper right. The eggs were then placed in a fluorescence microscope for an initial period of imaging at 37 °C (imaging #1) that began shortly after the addition of Chol/MβCD. Relative $[Ca^{2+}]_i$ measured using an inverted microscope as a function of time was determined as the ratio of fluorescence intensities excited by 340-nm and 380-nm light [sequentially excited every (*A*) 5 or (*B*) 60 s]. After 25 min of Chol/MβCD exposure, the eggs were washed and placed in Chol/MβCD-free M2 medium and repositioned in the microscope, and the imaging continued for an additional (*A*) 15 min or (*B*) ~2.5 h at 37 °C (imaging #2). Fluorescence data could not be collected during the 5–10 min required to wash away the Chol/MβCD, position, and refocus on the eggs for additional imaging in Chol/MβCD-free medium (indicated by dotted lines in the diagram in the upper right). In *A*, we present some of the data from a subset of eggs treated with Chol/MβCD ($n = 4$), in which the peak of $[Ca^{2+}]_i$ occurred before the wash period from one untreated control egg (blue). Slight experiment to experiment variations in the times at which imaging began or ended are indicated by wavy lines in the diagram in the upper right. After imaging, eggs were cultured in Chol/MβCD-free M2 medium at 37 °C for an additional ~5–24 h to assess second PB extrusion and cleavage to the two-cell stage. *B* shows results for four representative individual eggs treated with Chol/MβCD and one (blue) of four untreated control eggs from the same experiment. Second PB extrusion was assessed at the end of the imaging period.

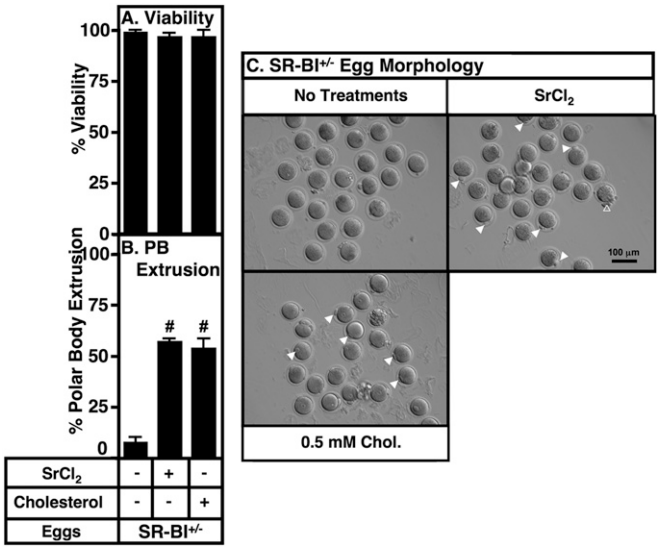

Fig. S7. Effects of the cholesterol loading on viability and activation of control *SR-BI*$^{+/-}$ eggs. Eggs from *SR-BI*$^{+/-}$ mice harvested ~16 h after hCG administration (induction of superovulation) in three independent experiments were denuded by hyaluronidase treatment. All eggs were then preincubated for 15 min at 37 °C in M16 medium without (–) or with (+) 0.5 mM cholesterol-loaded MβCD (cholesterol) and then washed one time in M16 medium. The oocytes were then incubated for 6 h in M16 medium at 37 °C in the absence (–) or presence (+) of 5 mM $SrCl_2$/2 mM EGTA. The total numbers of oocytes examined were 105 (untreated), 88 ($SrCl_2$/EGTA), and 90 (cholesterol). After 6 h of incubation, we determined (*A*) the percentage of oocytes that remained viable and (*B*) the percentage of those oocytes exhibiting second PB extrusion. The values for one-way ANOVA were (*A*) $P = 0.86$ and (*B*) $P \leq 0.0001$. $SrCl_2$/EGTA and cholesterol treatments both yielded statistically significant differences in PB extrusion compared with the untreated *SR-BI*$^{+/-}$ control as indicated. $^{\#}P < 0.001$ (posthoc Tukey test). (*C*) The oocytes were visualized using phase contrast microscopy. Solid white arrowheads indicate PBs, and open arrowhead indicates cumulus cells. (Magnification: 100×. Scale bar: 100 μm.)

Table S1. Completion of MI

Genotype	GV* (%)	GVBD (%)	First PB extruded (%)	*n*
SR-BI$^{+/-}$	13	87	78	76
SR-BI$^{-/-}$	26	74	64	77

*Oocytes at the GV stage surrounded by cumulus cells were collected from unprimed 6- to 8-wk-old female mice after follicular puncture in collection medium as described in *SI Materials and Methods*. Oocytes were then cultured for 14 h in basal in vitro maturation medium. The oocytes were fixed in microtubule stabilizing buffer, DNA was stained with Hoechst 33258 dye, and images were collected using light and fluorescence microscopy to assess meiotic maturation (*SI Materials and Methods*).